*Macromolecules* **1980,** *13,* 1495–1501

# Dielectric and Mechanical Relaxations in Randomly Coupled Multiblock Copolymers with Varying Block Lengths: Bisphenol-A Polycarbonate–Poly(oxyethylene) Systems

**Toshitake Suzuki and Tadao Kotaka***

*Department of Polymer Science, Faculty of Science, Osaka University,*
*Toyonaka, Osaka 560, Japan.* *Received March 11, 1980*

ABSTRACT: For $(AB)_n$ multiblock copolymers of bisphenol-A polycarbonate (PC) and poly(oxyethylene) (POE) with varying block lengths $X$ and $Y$, respectively, the dependence on block lengths of crystallization and melting, microphase separation, and relaxation behavior were examined by DSC, dynamic viscoelastic, and dielectric relaxation measurements. The crystallization of POE blocks is hampered by the adjoining hard PC blocks, while that of PC blocks is facilitated by the soft POE blocks. In the samples with relatively long block lengths ($X \gtrsim 5$ and $Y \gtrsim 20$), semicrystalline PC and amorphous POE domains and a small amount of POE/PC intermixing domains may coexist. These copolymers show block copolymer behavior. In those copolymers with intermediate block lengths ($X \simeq$ 3–5 and $20 \gtrsim Y \gtrsim 8$), semicrystalline PC domains may coexist with POE/PC intermixing domains. The copolymers with short block lengths ($X \lesssim 2$ and $Y \lesssim 4$) exhibit single-phase random copolymer behavior. Yet the low-temperature, high-frequency dielectric $\beta$ relaxation of the copolymers, irrespective of the block lengths, preserves the characteristics of the local in-chain motions of the POE homopolymers.

Recently there has been an increasing interest in the studies of the structure and properties of multicomponent polymers or polymeric alloys.[1,2] These materials exhibit unique physical properties on account of the microphase separation between the constituent polymers. Alternating $(AB)_n$-type multiblock copolymers, such as segmented polyurethane elastomers,[3-5] also belong to this class of materials when the block lengths are sufficiently long to induce microphase separation. The $(AB)_n$-type multiblock copolymers are usually synthesized by the condensation of different bifunctional oligomers.[6] In such systems the relative incompatibility and hence the microphase separation behavior depend not only on the chemical nature of the oligomers but also on other factors, such as the block lengths, the number of blocks in a chain, and the overall composition.[7-9] When either one or both of the blocks are crystallizable, the microphase separation proceeds more easily, even when the block lengths are relatively short.[10] We expect that the properties of a multiblock copolymer would vary from homogeneous random copolymer properties to heterophase block copolymer properties with increasing block lengths. In addition to these expectations, a multiblock copolymer composed of soft amorphous segments (or crystalline segments but with a low melting temperature) and hard crystalline segments would provide an interesting model system by which we can study the influence of the hard segments on the molecular motions of the adjoining soft segments and vice versa. Such knowledge would enrich our understanding on the relaxation behavior of homopolymer molecules in general.

We attempted to examine, along these lines, the behavior of a multiblock copolymer composed of soft- and hard-segment blocks with varying lengths. To this end we selected a multiblock copolymer composed of poly(oxyethylene) (POE) and bisphenol-A polycarbonate (PC) segments[11,12] as a model system. We prepared two series of well-defined samples: In one series of the PC-block length was kept constant while the other was varied. In the other series the PC/POE ratio was kept constant while their lengths were varied. On these materials we carried out differential scanning calorimetry (DSC), dielectric, and dynamic mechanical measurements.[13,14] We report the results herein.

## Experimental Section

**Materials.** Poly(oxyethylene glycols) and bisphenol-A were commercially available materials and were purified as follows. Bisphenol-A was recrystallized from benzene/methanol (volume ratio 100:5) mixture. Poly(oxyethylene glycols) with nominal molecular weights of 3000 and 1000 were purified by fractional recrystallization from toluene solution. The other three poly(oxyethylene glycols) with $M$ = 600, 400, and 300 and tetrakis(oxyethylene glycol) ($M$ = 194) were fractionally precipitated from benzene solution by $n$-hexane. Bis(oxyethylene glycol) ($M$ = 106) was simply washed with benzene. These purified polyethers were examined on a gel permeation chromatograph (GPC) (Model HLC-801A, Toyo Soda Mfg. Co.) and found to have narrow molecular weight distributions.

Block copolymerization was carried out according to the procedure reported by Goldberg.[12] Prescribed amounts of bisphenol-A (B) and poly(oxyethylene glycol) were mixed in pyridine, into which phosgene was introduced with vigorous stirring while the temperature was kept below 30 °C. The product was recovered by adding excess 2-propanol and further washed several times with 2-propanol. The product was then dissolved in tetrahydrofuran to make a 5% solution and reprecipitated by pouring it into excess hexane. The procedure was repeated three times. Finally powder-form precipitates were dried under vacuum at 60 °C. The details of the procedure were slightly modified from sample to sample, depending on their compositions and block lengths.[13,14]

The composition of the product was determined by elemental analysis and by UV absorption. Average molecular weight was estimated on the Toyo Soda GPC equipped with a refractometer and a UV-absorption monitor. The carrier solvent was tetrahydrofuran. Narrow-distribution polystyrenes and poly(oxyethylene glycols) were used as the elution standards.

The characteristics of the copolymer samples are summarized in Table I, in which the samples are coded as B$X$E$Y$: the symbols $X$ and $Y$ denoted, respectively, the average degree of polymerization of a PC block and that of the POE precursor. The average number $Z$ of the POE oligomers coupled to form a POE block and the value of $X$ were calculated with an assumption of random coupling of the $B$ units and the POE oligomers from the monomer feeds and product compositions. In series I the PC-block length was kept constant ($X \simeq 5$), while the POE-block length was varied from $Y = 2$ to $Y = 23$ (or more precisely, $YZ \simeq$ 2.4–27.6). In series II the POE/PC ratio was kept constant (roughly 37/63 by weight), while $X$ was varied from about 2 to 20 and $Y$ from 4 to 63 (or $YZ$ from 6.4 to 74.8).

**Methods.** The copolymer samples were molded into films of 0.3–0.5-mm thickness by a hot press above their respective softening temperatures (100–200 °C range) and subsequently heat treated whenever necessary.[13,14] Dielectric measurements were made in the 3.125–100-kHz range on a capacitance bridge (General Radio Model 1615A), a Cole-Gross bridge (Showa Denki Labs., Tokyo, Model S-1), and an automatic capacitance bridge (Yokogawa-Hewlett-Packard Model YHP 4070A). A specimen with a 30-mm diameter was inserted in a homemade three-electrode

0024-9297/80/2213-1495$01.00/0

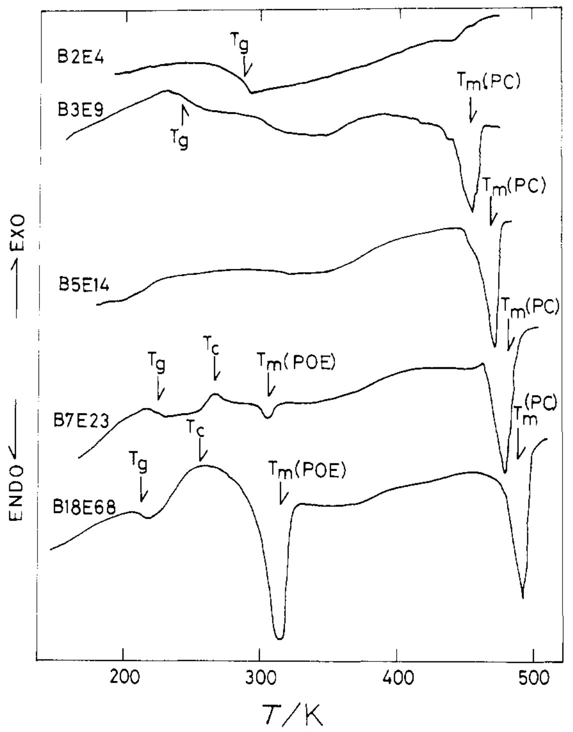

**Figure 1.** Differential scanning calorimetric thermograms of series II samples. The measurements were made with a heating rate of 10 K $\text{min}^{-1}$.

cell with a brass sealing container.[13-15] Before measurements, the specimen was dried in situ at about $10^{-2}$ torr for 12 h, and the atmosphere in the container was replaced by helium to avoid moisture. Dynamic mechanical measurements were usually made on a Rheovibron DDV-II (Toyo-Baldwin Co.) at 110 Hz in the temperature range from 150 to 450 K. Differential scanning calorimetry was usually carried out on a DSC (Rigaku Denki Co., Model 8055) in the range from 210 to 573 K with a heating rate of 10 K $\text{min}^{-1}$.

## Results

**Differential Scanning Calorimetry.** Figure 1 shows some examples of DSC thermograms of the series II samples. The endothermic peak due to the melting of PC crystallites was observed in the range from 470 to 500 K except for B2E4. When the specimens were quenched from 493 K, which was slightly above the melting temperature $T_m$ of the PC crystallites, the PC-melting peaks were no longer observed except for those of B5E14, B5E23, B7E23, and B18E68. Interestingly, in these quenched specimens the PC-melting peaks in the 470–490 K range were always preceded by exothermic peaks in the range 355–400 K, which were apparently due to the recrystallization of PC blocks during the reheating process. Particularly in the quenched specimen of B5E23, the PC recrystallization appears to be much easier. For example, annealing at room temperature for 1 h diminishes the PC-recrystallization peak and only the melting peak appears.

The exo- and endothermic peaks due to the crystallization and melting of POE crystallites were observed at about 270 and 303 K, respectively, for the B5E23, B7E23, and B18E68 samples, all of which have relatively long POE blocks. When these samples were annealed at 273 K, the area under the POE-melting peak grew larger.

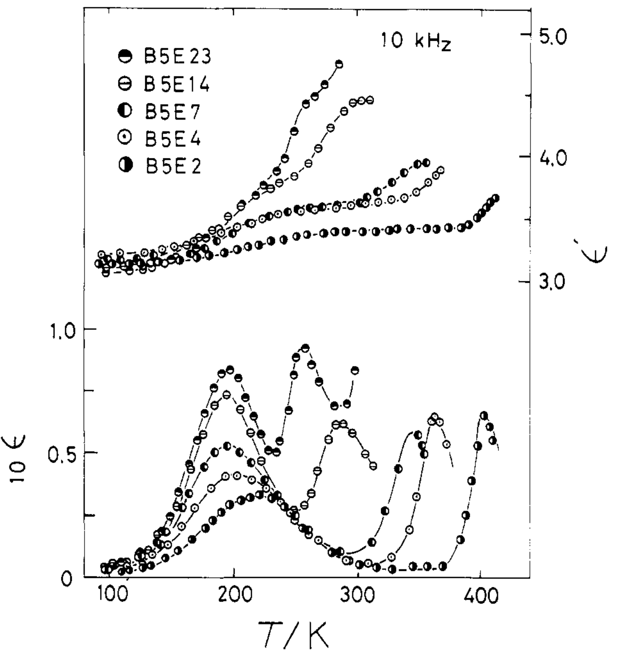

**Figure 2.** Temperature dependence of dielectric permittivity $\epsilon'$ and loss $\epsilon''$ measured at 10 kHz on series I samples.

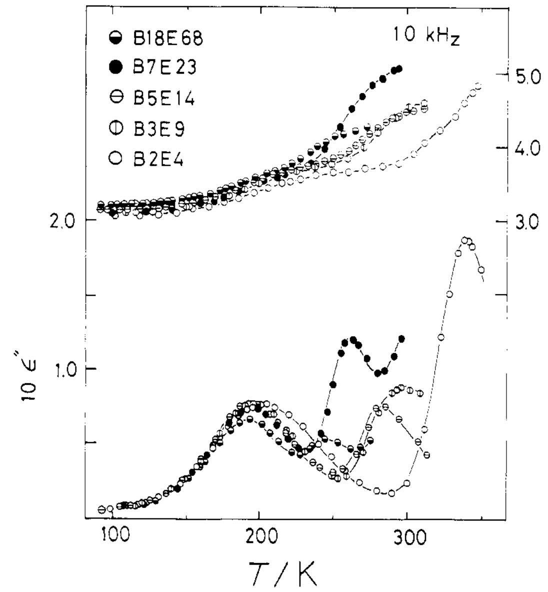

**Figure 3.** Temperature dependence of $\epsilon'$ and $\epsilon''$ measured at 10 kHz on series II samples.

Glass transition was detected as an endothermic shift in DSC thermograms for all samples except B5E14 and B3E9. Gradual change in the slope of the thermograms of these samples implies a broad transition region. The glass transition temperature $T_g$ became lower with increasing POE-block length or POE content and finally approached that of the POE homopolymers (about 220 K).[16] Another interesting observation was that the specimens quenched from 493 K always showed a somewhat higher $T_g$ than that of the corresponding annealed specimens (or more precisely those slowly cooled from the temperature which is just below the $T_m$ of each PC crystallite). Table II summarizes the results of the DSC measurements.

**Dielectric Properties.** Figures 2 and 3 show the temperature dependence of dielectric permittivity $\epsilon'$ and loss $\epsilon''$ measured at 10 kHz for the series I and II samples, respectively. In the loss curves there are two peaks and they are designated $\alpha$ and $\beta$ from the high-temperature side.[17,18] Apparently the $\alpha$-peak temperature $T_\alpha$ decreases with increasing POE-block length or POE content, corresponding to $T_g$ as determined by the DSC method. On the other hand, the $\beta$-peak temperature $T_\beta$ is almost independent of POE-block length and remains nearly the same

Table I
Characteristics of the Copolymer Samples

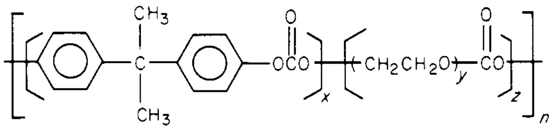

| sample code (B*X*E*Y*) | bisphenol-A content in monomer feed, wt % | bisphenol-A carbonate content, wt % | $X^a$ | $Y^b$ | $Z^a$ | $n^b$ |
|---|---|---|---|---|---|---|
| | | Series I Samples | | | | |
| B5E23 | 48.5 | 49.8 | 5.1 | 23 | 1.2 | 7 |
| B5E14 | 61.3 | 67.5 | 6.5 | 14 | 1.2 | 12 |
| B5E7 | 75.8 | 78.3 | 6.0 | 7 | 1.2 | 15 |
| B5E4 | 82.2 | 85.2 | 6.0 | 4 | 1.2 | 8 |
| B5E2 | 89.5 | 90.2 | 5.8 | 2 | 1.2 | 16 |
| | | Series II Samples | | | | |
| B18E68 | 62.5 | 60.7 | 19.3 | 68 | 1.1 | 2 |
| B7E23 | 62.5 | 64.3 | 8.4 | 23 | 1.1 | 3 |
| B5E14[c] | | | | | | |
| B3E9 | 62.5 | 65.4 | 4.3 | 9 | 1.3 | 16 |
| B2E4 | 62.5 | 66.9 | 2.7 | 4 | 1.6 | 25 |

[a] Determined from PC content by elemental analysis. [b] Determined from GPC data. [c] The same sample as in series I.

Table II
Summary of DSC Data of the Copolymer Samples[a]

| code | annealed specimens | | | quenched specimens | | |
|---|---|---|---|---|---|---|
| (B*X*E*Y*) | $T_g$ | $T_m^{POE}$ ($X_c$/%) | $T_m^{PC}$ ($X_c$/%) | $T_g$ | $T_m^{PC}$ | $T_c^{PC}$ |
| B5E23 | 231 | 303 (16) | 474 (11) | 235 | 469 | 355[b] |
| B5E14 | 268[c] | | 483 (23) | 304 | 472 | 380 |
| B5E7 | 311 | | 479 (20) | 340 | | |
| B5E4 | 331 | | 476 (21) | 352 | | |
| B5E2 | 380 | | 480 (17) | 384 | | |
| B18E68 | 223 | 307 (19) | 494 (21) | 225 | 496 | 398 |
| B7E23 | 231 | 303 (2) | 483 (20) | 278 | 477 | 387 |
| B3E9 | 260[d] | | 467 (14) | 296 | | |
| B2E4 | 300 | | | 299 | | |

[a] Crystalline melting ($T_m$) and glass transition ($T_g$) temperatures for the homopolymers are as follows: $T_m^{PC}$ = 522 K, $T_g^{PC}$ = 418 K, $T_m^{POE}$ = 303 K, $T_g^{POE}$ = 220 K. $X_c$ is the degree of crystallinity in wt % determined from the DSC melting peak area. [b] This crystallization peak at $T_c$ appears immediately after the quenching. The peak dissappears after 2 h of annealing at room temperature. [c] From ε″ data. [d] Not clearly observed.

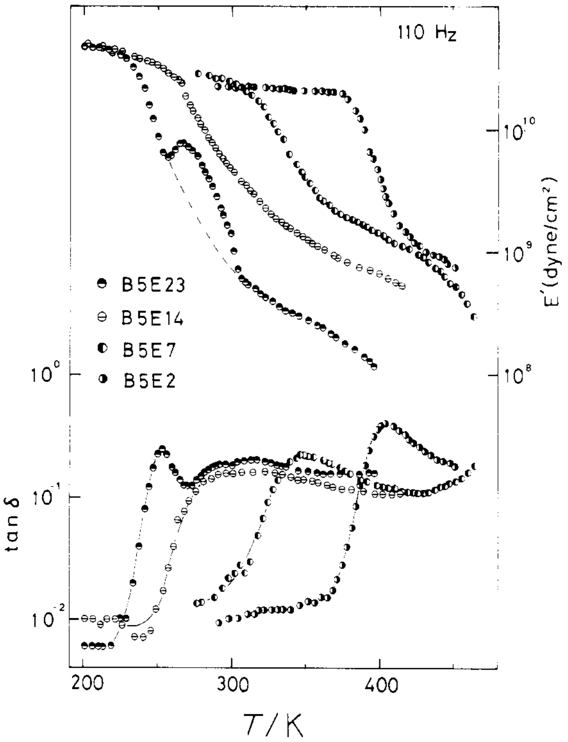

**Figure 4.** Temperature dependence of the storage Young's modulus $E'$ and loss tan δ measured at 110 Hz on series I samples.

as that of the POE homopolymers.[19] However, as the POE blocks become as short as the dimers, the $T_\beta$ begins to shift to slightly higher temperature (cf. Figure 2, B5E2). The area under the β peak varies roughly in proportion to the overall POE content.

Plots of log (frequency *f*) vs. $T_\alpha^{-1}$ were all of the Williams–Landel–Ferry (WLF) equation[20] type. From the slopes of the plots at 10 kHz, the activation energy $\Delta E_\alpha$ was found to vary from about 540 kJ mol$^{-1}$ for B5E2 to 290 kJ mol$^{-1}$ for B5E23 as the PC content decreased. These values are comparable, respectively, to those of the PC and POE homopolymers.[19,21] On the other hand, similar plots for the β relaxation were all of the Arrhenius equation[17] type, giving nearly the same activation energy $\Delta E_\beta$ value of about 42 kJ mol$^{-1}$ for all the samples. This value is comparable to that of the POE homopolymers.[19]

**Dynamic Mechanical Properties.** Figures 4 and 5 show the temperature dependence of the storage Young's modulus $E'$ and mechanical loss tan δ for the series I and II samples, respectively. In Figure 5, each curve was successively shifted upward by 1 decade starting from that of the B2E4 sample for the sake of comparison. In all the curves the mechanical α relaxation is observed in the region which corresponds to the DSC $T_g$ and dielectric $T_\alpha$ regions. Their behavior may be classified into two groups: One group contains samples B2E4 and B5E2, which exhibit a single-transition region where $E'$ drops sharply around 320 and 390 K, respectively. The other group contains those samples which exhibit a broad transition region where $E'$ decreases slowly and tan δ becomes almost a plateau, as seen for B5E23, B7E23, and B18E68. The onset of the transition in the latter group roughly corresponds to that of the POE homopolymers.

The temperature dispersion curves of the B5E23 and B18E68 samples show anomalous behavior in the 270–300 K range. The anomaly appears to correspond to the initiation of crystallization and remelting of POE domains,

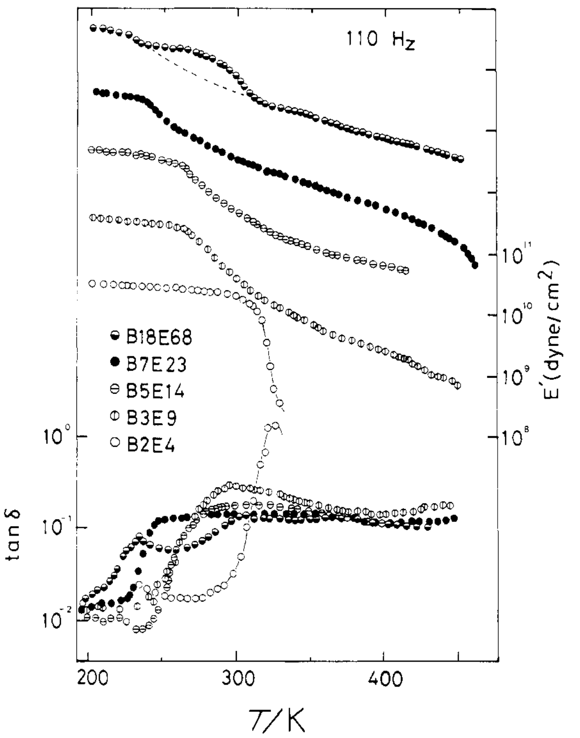

**Figure 5.** Temperature dependence of $E'$ and tan $\delta$ measured at 110 Hz on series II samples.

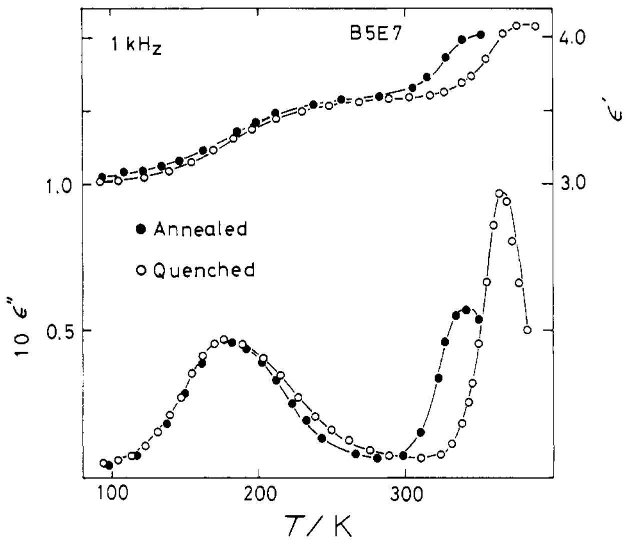

**Figure 6.** Effect of thermal treatment on the temperature-dependence curves of $\epsilon'$ and $\epsilon''$ measured at 1 kHz on B5E7.

as has also been observed in the DSC thermograms. Interestingly, if these samples are cooled from a high temperature to a temperature slightly below $T_m$ but above the crystallization temperature $T_c$ of the POE crystallites, the anomaly disappears and the $E'$ curve follows the dashed line in Figures 4 and 5.

**Effects of Thermal Treatments.** As judged from the DSC and other data, thermal treatments exert profound influence on the sample morphologies and hence the properties. For example, annealing of the B5E23 specimen at 273 K increases the degree of crystallinity in the POE blocks. Also the DSC data of annealed specimens and those quenched from 493 K suggest that these samples may assume different morphologies by such thermal treatments. We compared the properties of these specimens for the same samples. Figure 6 compares the temperature dependence of $\epsilon'$ and $\epsilon''$ of the annealed and quenched specimens of the B5E7 sample, while Figure 7 compares $E'$ and tan $\delta$. In Figure 6 we notice that quenching resulted in a rise of $T_\alpha$ but produced virtually no effect on the $\beta$-relaxation process. On the other hand, in Figure 7 we notice the mechanical $\alpha$-relaxation behavior was changed from semicrystalline polymer behavior to homogeneous random-copolymer behavior.

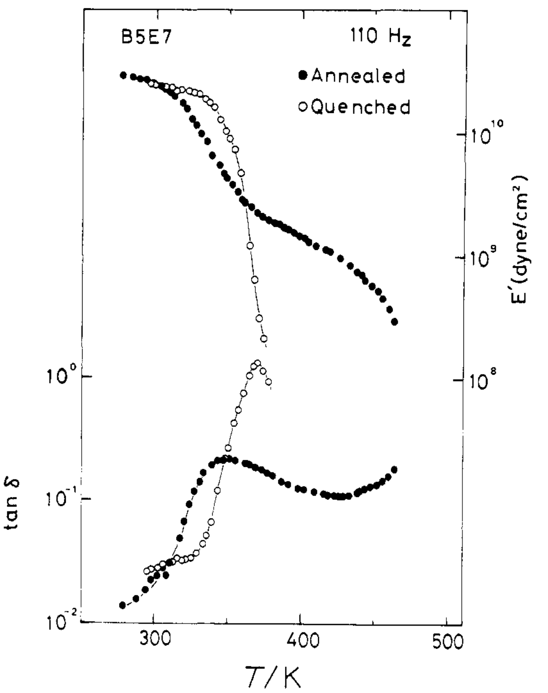

**Figure 7.** Effect of thermal treatment on the temperature-dependence curves of $E'$ and tan $\delta$ measured at 110 Hz on B5E7.

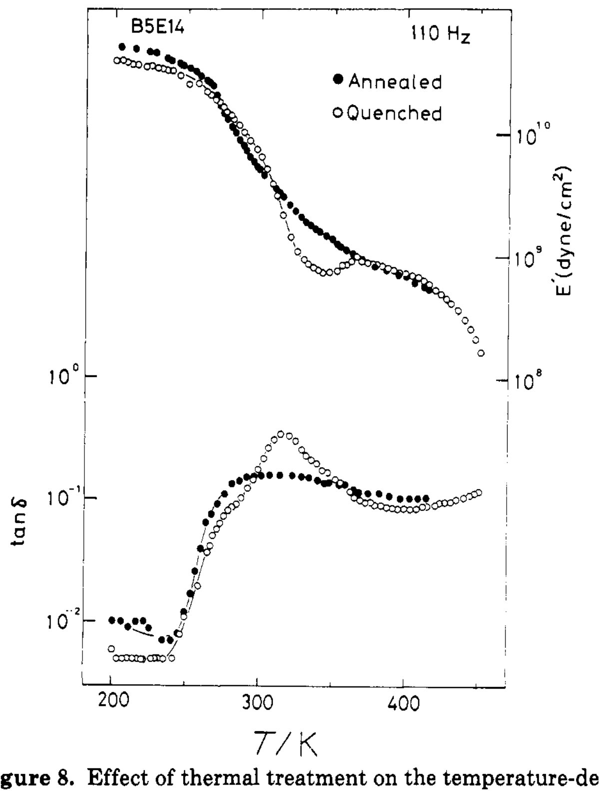

**Figure 8.** Effect of thermal treatment on the temperature-dependence curves of $E'$ and tan $\delta$ measured at 110 Hz on B5E14.

In Figure 8 we compare the temperature dependence of $E'$ and tan $\delta$ of the annealed and quenched specimens of the B5E14 sample. The former shows a gradual decrease in $E'$ and a plateau in tan $\delta$, corresponding to the broad

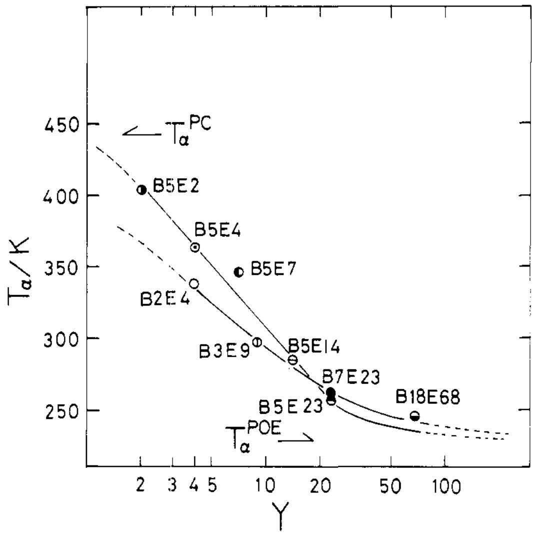

**Figure 9.** Dependence on POE block length $Y$ of dielectric $\alpha$-transition temperature $T_\alpha$ of series I and II samples.

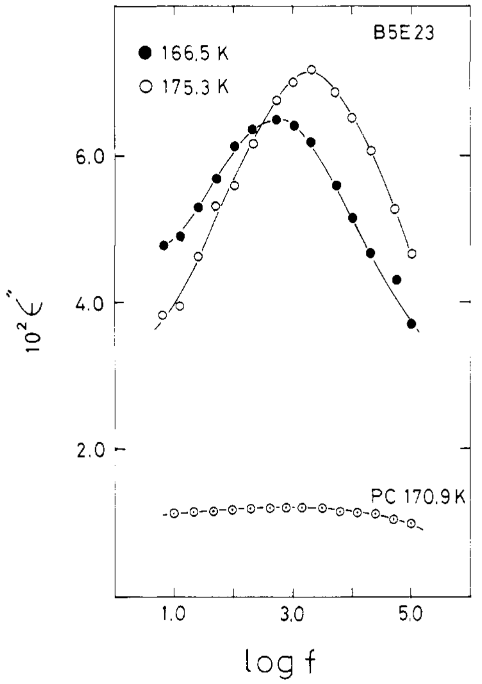

**Figure 10.** Frequency dependence of dielectric loss $\epsilon''$ in the $\beta$-transition region of B5E23 measured at 166.5 and 175.3 K and a similar curve for the PC homopolymer at 170.9 K.

transition region observed in the DSC thermograms. The latter, on the other hand, shows an anomalous rise in $E'$ around 340 K. This anomaly appears to be similar in nature to those observed in the B5E23 and B18E68 samples in the 270 and 300 K regions. However, for the quenched B5E14 specimen the anomaly must be due to the crystallization of PC blocks, while in the B5E23 and B18E68 samples of the crystallization of POE blocks is involved.

## Discussion

**Crystallization, Melting, and Glass Transition Behavior.** The experimental results described so far clearly indicate that the crystallization and melting behavior or the POE and PC blocks are strongly dependent on the block lengths. In general, the crystallization of soft POE blocks is hampered by the adjoining hard PC blocks, while that of hard PC blocks is facilitated by the adjoining soft POE blocks. For PC hompolymers it is known that the crystallization rate is slow and hence specimens quenched from the melt usually show no crystallinity even after the specimens have been annealed.[22] Nevertheless the quenched specimens of the B5E14, B5E23, B7E23, and B18E68 samples always show DSC PC-melting peaks in the range 470–490 K, which are preceded by PC-crystallization peaks in the range 350–400 K. In the series II samples a considerable decrease in $T_m$ is observed with decreased PC-block length, and finally in B2E4 no crystallization takes place. Two reasons are responsible for this behavior: the average size of the PC crystallities becomes smaller, and the microphase separation between the PC and POE blocks becomes less complete, thereby forming a POE/PC intermixing phase in the sample as the PC-block length becomes shorter.

The existence of such a POE/PC intermixing phase is evident also from the fact that quenched specimens always show higher $T_g$ or $T_\alpha$ than annealed specimens of the corresponding samples (cf. Table II). The quenching reduces the degree of crystallinity in the PC blocks and increases the relative concentration of PC in the intermixing phase. An exception is B2E4, in which no PC crystallites exist even in annealed specimens, and quenching does not alter the sample morphology.

Now turning our attention to the glass transition and the dielectric $\alpha$-relaxation behavior, we have plotted the $T_\alpha$ vs. the average POE-block length $Y$ (Figure 9). In the series I samples, $T_\alpha$ approaches that of the PC homopolymers $T_\alpha^{PC}$ ($\simeq$445 K),[21] while in the series II samples, $T_\alpha$ approaches that of a homogeneous random copolymer as estimated by the Gordon–Taylor[23] or the Fox[24] equation, with decreasing POE-block length $Y$. On the other hand, with increasing $Y$ (>20), $T_\alpha$ approaches that of the POE homopolymer $T_\alpha^{POE}$ ($\simeq$220–230 K).[19]

From these results we may conclude that the $\alpha$-relaxation process is associated with the glass transition of the copolymer amorphous domains, which approaches the so-called $\alpha_a$ relaxation[18] in the amorphous phase of the POE homopolymers. However, we failed to observe the $\alpha$ relaxation associated with the $\alpha_a$ relaxation in the PC domains. In PC homopolymers the glass transition appears at about 418 K.[22] In these copolymers, however, the dielectric $\alpha$-transition peaks might have been masked by ionic conduction current in more conductive POE domains.

**Interpretation of Dielectric $\beta$ Relaxation.** The dielectric $\beta$ relaxation of the copolymers is presumably a composite of the contributions from POE and PC segments. In the homopolymers the former is found at around 185 K and the latter around 195 K when observed at 10-kHz frequency.[17,19,21] Figure 10 shows the frequency dependence of $\epsilon''$ for B5E23 and a PC homopolymer[21] in the low-temperature region. Apparently the contribution from the PC blocks is small. From this and other data shown in Figures 2 and 3, we assigned the $\beta$ relaxation as due primarily to the local in-chain motions[17] of POE segments. This type of relaxation is usually labeled $\gamma$.[17] However, here we follow the convention proposed by Ishida,[18] who assigned the dielectric relaxations of semicrystalline polymers (having no polar side groups) as due to the crystalline phase ($\alpha_c$), the amorphous phase ($\alpha_a$), and the local in-chain motions ($\beta$), instead of $\alpha$, $\beta$, and $\gamma$ from high-temperature side.

The present data clearly indicate that POE segments of the size as small as a dimer or a sequence of five or six bonds can accommodate the intrachain motions involved in the $\beta$ relaxation. For such a low-temperature high-frequency relaxation Schatzki[25,27] and Boyer[26] proposed models based on *crankshaft* mechanisms[17] while Monnerie et al.[29,30] proposed *three-bond* and *four-bond* motions.

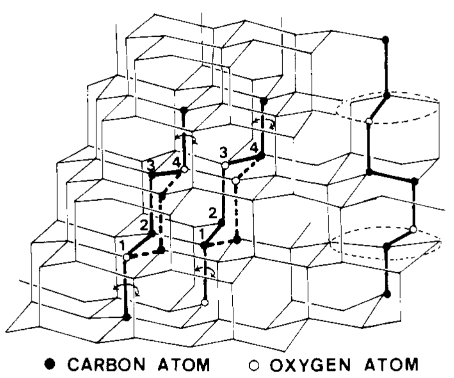

**Figure 11.** Two-site model representing tg$^+$t $\rightleftarrows$ tg$^-$t transitions in an oxyethylene dimer (left) and a Schatzki crankshaft model in an oxyethylene trimer (right).

Some of the models are illustrated in Figure 11 on a tetrahedral diamond-type lattice. In view of the rather large relaxation strength but the small scale of the local intrachain motions the Schatzki crankshaft, which has five intervening bonds between the collinear bonds (shafts), appears to be still too large in scale. Also the probability that a portion of a POE block can assume such a crankshaft is too small. On the other hand, the Boyer crankshaft has only three intervening bonds but involves the energetically unfavorable cis conformation, which cannot be fitted into the tetrahedral lattice. Moreover, both crankshafts appear to demand fairly large free volumes to complete the motions. Therefore a smaller scale motion will be preferable. Thus we employ a two-site model similar to Monnerie's *three-bond* motions and calculate the relaxation strength $\Delta\epsilon$ to see whether such a model would reasonably explain the $\beta$ relaxation of the copolymers.

The relaxation strength $\Delta\epsilon$ of any relaxation processes in polar polymers may be adequately given by applying the Onsager equation[31] to the two-site model

$$\Delta\epsilon = \frac{3\epsilon_S}{2\epsilon_S + \epsilon_\infty}\,\frac{\pi N\mu^2}{3kT}\left(\frac{\epsilon_\infty{}^2 + 2}{3}\right)^2 \quad (1)$$

Here $\epsilon_S$ and $\epsilon_\infty$ are the static and high-frequency values of the dielectric constant, respectively, and $N$ is the number (per unit volume) of motional units which shift back and forth between two sites possessing the vector difference $\mu$ in the dipole moments. The value of $\mu$ may be calculated, if an adequate value is assigned for the dipole moment of the motional units and the two sites are specifically defined. In this case we employed the value of ethyl ether molecules in the gas phase (1.1 D) for the dipole moment. Finally we have to define the two sites.

On a tetrahedral lattice any consecutive three bonds would assume any one of 27 conformations (trans–gauche$^+$–trans (tg$^+$t) etc.). Among these conformations, the two g$^+$g$^-$g$^+$ and g$^-$g$^+$g$^-$ form a cyclohexane structure and may be ruled out. We assume the remaining 25 conformations are equally probable. Then among the 25 conformations only the flip-flop transition tg$^+$t $\rightleftarrows$ tg$^-$t is possible by simultaneous rotations around the zeroth and fourth bonds without moving the rest of the chain (cf. Figure 11). The average number of tg$^+$t or tg$^-$t triads that would appear in a POE block of length $Y$ is $2(3Y - 4)/25$. Then the number $N$ is given by

$$N = (N_A\rho\omega_{POE}/m_{OE}Y)\{2(3Y - 4)/25\} \quad (2)$$

where $N_A$ is Avogadro's number, $\rho$ the sample density, $\omega_{POE}$ the POE content by weight fraction, and $m_{OE}$ the molar mass of an oxyethylene unit. The dipole moment difference $\mu$ may take two values: one is $\mu_I = 1.57$ D when the oxygen is either on the 2- or 3-position, and the other is $\mu_{II} = 3.14$ D when the two oxygens are on 1- and 4-positions (cf. Figure 11). The I conformations will appear twice and the II conformation once in every three tg$^+$t $\rightleftarrows$ tg$^-$t conformations. We must also consider the contribution of oxygen molecules at both ends of a POE block, which gives $\mu_{III} = 3.14$ D. Taking all these factors into account, we arrive at $N\mu^2$ for POE blocks in a unit volume as

$$N\mu^2 = \{[\tfrac{2}{3}(\mu_I)^2 + \tfrac{1}{3}(\mu_{II})^2][2(3Y - 4)/25] + 2(\mu_{III})^2\} \times (N_A\rho\omega_{POE}/m_{OE}Y) \quad (3)$$

Table III
Calculated and Observed Magnitudes $\Delta\epsilon$ of Dielectric Dispersion in the $\beta$-Relaxation Process

| code | obsd | calcd |
|---|---|---|
| B5E23 | 0.52 | 1.42 |
| B5E14 | 0.49 | 0.90 |
| B5E7 | 0.37 | 0.52 |
| B5E4 | 0.33 | 0.30 |
| B5E2 | 0.26 | 0.15 |
| B18E68 | 0.45 | 1.00 |
| B7E23 | 0.47 | 0.90 |
| B3E9 | 0.52 | 0.80 |
| B2E4 | 0.50 | 0.67 |

Inserting eq 3 into the Onsager equation (eq 1), we can estimate the $\Delta\epsilon$ values for the copolymer samples. The results are summarized in Table III. In spite of the crudeness of the two-site model employed here, we see that the calculated $\Delta\epsilon$ values are at least in the right order of magnitude for the observed values. For those with longer POE length the calculated values are larger by a factor of 2–3 than the observed values. This discrepancy might be due to that in long POE blocks the crystallization of the POE blocks might set the restriction even on the local in-chain motions and that the number of allowed tg$^+$t $\rightleftarrows$ tg$^-$t transition might be overestimated because the steric hindrances due to the folding back of remote bonds have been all neglected in the calculation. Incidentally Boyd and Breitling[28] calculated the activation energy of the tg$^+$t $\rightleftarrows$ tg$^-$t transition for polyethylene chain to be about 42–50 kJ mol$^{-1}$. This value is in agreement with $\Delta E_\beta$ for the present systems. This provides additional support for our speculation that the $\beta$-relaxation mechanism might be mainly due to the local tg$^+$t $\rightleftarrows$ tg$^-$t transition in the POE blocks.

## Conclusion

In summary, in the samples with relatively long block lengths (e.g., $X \gtrsim 5$ and $Y \gtrsim 20$), semicrystalline PC and amorphous POE domains and a small amount of POE/PC intermixing domains may coexist. These samples exhibit a transition near the glass transition $T_g{}^{POE}$ of the POE homopolymers and a subsequent gradual decrease in $E'$ and a plateau in tan $\delta$. The B5E23 and B18E68 samples show an anomaly in the 270–300 K region due to crystallization and remelting of the POE phase during the dynamic viscoelastic measurements. In those samples with intermediate block lengths (e.g., $X \simeq 3$–$5$ and $20 \gtrsim Y \gtrsim 8$), semicrystalline PC domains coexist with POE/PC intermixing domains. The PC crystallites easily melt into the intermixing phase and re-form after adequate annealing. These samples show a drop in $E'$ in the glass transition region of POE/PC intermixing phase and a subsequent gradual decrease in $E'$. The copolymers with short block lengths ($X \lesssim 2$ and $Y \lesssim 4$) exhibit a homogeneous, single-phase random-copolymer behavior, in which a sharp drop in $E'$ is seen in the region expected from the Gordon–Taylor or Fox equation for POE/PC intermixing

*Macromolecules* **1980**, *13*, 1501-1508 **1501**

phase. Yet the dielectric $\beta$ relaxation of the copolymers preserves the feature which is characteristic of POE homopolymers. The most likely mechanism of this $\beta$ relaxation might be the flip-flop transition between $tg^+t \rightleftarrows tg^-t$ conformations in the POE blocks.

**Acknowledgment.** We thank Mr. Tatsuya Tamaki and Dr. Keiichiro Adachi of this laboratory for their assistance in carrying out the experiments. The work was supported in part by the Ministry of Education, Science and Culture, under the Grant-in-Aid program for 1976–1977 (Grant B147087).

### References and Notes

(1) Shen, M.; Kawai, H. *AIChE J.* **1978**, *24*, 1.
(2) Kotaka, T., Shen, M., Eds.; Proceedings of the U.S.–Japan Joint Seminar on Multicomponent Polymers, Kyoto, 1978 (*J. Macromol. Sci., Phys.*, in press).
(3) Manson, J. A.; Sperling, L. H. "Polymer Blends and Composites"; Plenum Press: New York, 1977; Chapter 5.
(4) Von Bogart, J. W. C.; Lilaonitkul, A.; Cooper, S. L. *Adv. Chem. Ser.* **1979**, *No. 179*.
(5) Cooper, S. L. Preprints, U.S.–Japan Joint Seminar on Multicomponent Polymers; Shen, M., Kotaka, T., Eds.; Kyoto, 1978.
(6) Noshay, A.; McGrath, J. E. "Block Copolymers"; Academic Press: New York, 1977; Chapter 7, p 305.
(7) Krause, S. *J. Polym. Sci., Part A-2* **1969**, *7*, 249.
(8) Krause, S. *Macromolecules* **1970**, *3*, 84.
(9) Krause, S. In "Colloidal and Morphological Behavior of Block and Graft Copolymers"; Molau, G., Ed.; Plenum Press: New York, 1971; pp 223–34.
(10) Krause, S. In "Block and Graft Copolymers"; Burke, J. J., Weiss, V., Eds.; Syracuse University Press: Syracuse, N.Y., 1973; pp 143–55.
(11) Merrill, S. H. *J. Polym. Sci.* **1961**, *55*, 343.
(12) Goldberg, E. P. *J. Polym. Sci., Part C* **1964**, *4*, 707.
(13) Suzuki. T. MS Dissertation, Osaka University, 1978.
(14) Suzuki, T.; Adachi, K.; Kotaka, T. *Rep. Prog. Polym. Phys. Jpn.* **1978**, *21*, 333.
(15) Adachi, K.; Hirose, Y.; Ishida, Y. *J. Polym. Sci.* **1975**, *13*, 737.
(16) Faucher, J. A.; Koleske, J. V.; Santee, E. R.; Stratta, J. J.; Wilson, C. W. *J. Appl. Phys.* **1966**, *37*, 3962. Faucher, J. A.; Koleske, J. V. *Polymer* **1968**, *9*, 44.
(17) McCrum, N. G.; Read, B. E.; Williams, G. "Anelastic and Dielectric Effects in Polymeric Solids"; Wiley: New York, 1967.
(18) Ishida, Y. *J. Polym. Sci., Part A-2* **1969**, *7*, 1835.
(19) Se, K.; Adachi, K.; Ishida, Y.; Kotaka, T. *Rep. Prog. Polym. Phys. Jpn.* **1977**, *20*, 375.
(20) Williams, M. L.; Landel, R. F.; Ferry, J. D. *J. Am. Chem. Soc.* **1955**, *77*, 3701.
(21) Matsuoka, S.; Ishida, Y. *J. Polym. Sci., Part C* **1966**, *14*, 247.
(22) Mercier, J. P.; Aklonis, J. J.; Litt, M.; Tobolsky, A. V. *J. Appl. Polym. Sci.* **1965**, *9*, 447.
(23) Gordon, M.; Taylor, T. S. *J. Appl. Chem.* **1952**, *2*, 493.
(24) Fox, T. G.; Loshaek, S. *J. Polym. Sci.* **1955**, *15*, 371.
(25) Schatzki, T. F. *J. Polym. Sci.* **1962**, *57*, 496.
(26) Boyer, R. F. *Rubber Chem. Technol.* **1963**, *34*, 1303.
(27) Schatzki, T. F. *Polym. Prepr., Am. Chem. Soc., Div. Polym. Chem.* **1965**, *6*, 646.
(28) Boyd, R. H.; Breitling, S. M. *Macromolecules* **1974**, *7*, 855.
(29) Valeur, B.; Jarry, J.-P.; Geny, F.; Monnerie, L *J. Polym. Sci., Polym. Phys. Ed.* **1975**, *13*, 667.
(30) Valeur, B.; Monnerie, L.; Jarry, J.-P. *J. Polym. Sci., Polym. Phys. Ed.* **1975**, *13*, 675.
(31) Onsager, L. *J. Am. Chem. Soc.* **1936**, *58*, 1486.

---

# On the Statistical Thermodynamics of Multicomponent Fluids: Equation of State

**R. K. Jain and Robert Simha***

*Department of Macromolecular Science, Case Western Reserve University, Cleveland, Ohio 44106.* *Received June 10, 1980*

ABSTRACT: The theory previously formulated and applied to homogeneous fluids of high and low molecular weights is generalized to multicomponent systems. The configurational free energy and equation of state retain the form derived for the homogeneous liquid with the characteristic parameters now functions of composition. Hence previous conclusions regarding an effective principle of corresponding states remain valid for mixtures of varying composition. When the scaling parameters for the separate components have been derived from *PVT* studies and the experimental isobar of the mixture at atmospheric pressure has been analyzed, the isotherms of the latter can be predicted without further recourse to experiment. The first applications of the theory are made to two series of binary mixtures of low molecular weight compounds. One is the *n*-hexane + *n*-hexadecane pair. Satisfactory agreement with experiment for the components and mixtures results at atmospheric and elevated pressures ($P \lesssim 5$ kbar). The results are combined with the information for polyethylene already available to compute the increase in the thermal expansivity of the polymer upon the addition of varying amounts of $n$-$C_{16}$. The second example is the $CCl_4 + C_6H_{12}$ system, where the former component had previously been analyzed. Good agreement with experiment is obtained for the equation of state of the second member and similarly for the series of mixtures at atmospheric pressure. Finally predictions for the elevated-pressure behavior of the latter are presented.

## Introduction

In recent years we have been concerned with the configurational thermodynamic properties of polymer and oligomer melts.[1,2] Most recently organic solvents have also been studied.[3] The analysis of the *PVT* properties followed a theory of the liquid state[4] based on the cell model modified by the introduction of a volume- and a temperature-dependent structure function in the form of vacancies (holes) in the quasi-lattice. This function is determined by the extremization of a configurational partition function.

The resulting equation of state has been quantitatively successful in the three types of fluids examined, i.e., amorphous high polymers, oligomers, and organic solvents, at atmospheric pressure as well as elevated pressures. The purpose of this paper is to report on a generalization of the theory to multicomponent fluids and on the first applications to mixtures of *n*-paraffins and of organic solvents. High polymer blends are not included.

## Recapitulation: The Homogeneous Fluid

The characteristic parameters of the system are defined in terms of the *equivalent s*-mer.[1] The relation between the *s*-mer and the real chain, the *n*-mer, i.e., the definition of the segment of the former in terms of the repeat unit of the latter, is derived from the experimental equation